

## Blends of Biphasic Ionomers with Chemically Identical Mono- and Bifunctional Oligomers

Michel Plante,<sup>†</sup> C. Geraldine Bazuin,<sup>\*,†</sup> and Robert Jérôme<sup>‡</sup>

Centre de Recherche en Sciences et Ingénierie des Macromolécules (CERSIM), Département de Chimie, Université Laval, Québec, Canada G1K 7P4, and Centre d'Étude et de Recherche sur les Macromolécules (CERM), Institut de Chimie, Université de Liège, B6, Sart-Tilman, 4000 Liège, Belgium

Received January 17, 1995; Revised Manuscript Received May 3, 1995\*

**ABSTRACT:** Biphasic Cs and Ba carboxylated polystyrene ionomers were blended with chemically identical mono- and bifunctional oligomers whose chain lengths are significantly greater than the average segmental length between ionic groups in the ionomer. The ionomers were chosen to have two ion contents such that, in one case, the matrix phase is dominant and, in the other, the cluster phase is dominant. From dynamic mechanical thermal analysis, it was observed that the biphasic morphology of the ionomers is preserved in all blends (containing up to 60 wt % oligomer). The monofunctional oligomers tend to have a mild plasticizing action on the two phases. In the matrix-dominated ionomer, the bifunctional oligomer has an antiplasticization effect at lower oligomer contents; this is attributed to a greater dispersion of ionic aggregates in the matrix phase, accompanied by pinning of the oligomer extremities in multiplets, which prevents plasticizing action. In the cluster-dominated ionomer, the oligomer forms a separate phase, which is related to insufficiently large ion-poor styrene regions in the ionomer to accommodate the long nonionic portion of the oligomer chains.

### Introduction

Several authors have drawn analogies between the widely-studied blends of a block copolymer with a homopolymer that is identical to or miscible with one of the blocks and blends of a biphasic ionomer with its parent homopolymer or with another polymer which is miscible with the parent homopolymer.<sup>1-3</sup> A parameter that plays an important role in determining the miscibility of block copolymer/homopolymer blends is the molecular weight of the homopolymer compared to the block with which it is, in principle, miscible. Similarly, for ionomers, the molecular weight of the homopolymer compared to the average molecular weight between ionic groups (or, inversely, the ion content) is important. In both cases, immiscibility results when the homopolymer molecular weight significantly exceeds the copolymer block length or ionomer equivalent weight. By extension, this parameter must also strongly influence blends of (chemically identical) block copolymers with significantly different block lengths and blends of (chemically identical) ionomers with significantly different ion contents. Of course, the strong tendency for ionic groups in ionomers to microphase separate from the organic matrix in order to minimize the energy of the system is also important to the miscibility of ionomer blends and may offset the molecular weight effect.

In order to explore the influence of these parameters in chemically identical ionomer blends, we have chosen to concentrate on a system where one of the ionomers is actually a functionalized oligomer or telechelic ionomer. The length of the chains in these ionomers is precisely defined. In a previous paper, we reported a study of biphasic carboxylated polystyrene ionomers (both Cs- and Ba-neutralized) blended with chemically identical, short, monofunctional polystyrene oligomers.<sup>4</sup> The length of these oligomers, composed of 8 styrene units, was about half that of the average segmental

length between ionic groups in the ionomers (where the ion content was 7 mol %, compared to 12.5 mol % in the oligomers) and about twice the estimated persistence length of polystyrene.<sup>4,5</sup> Plasticizing action by the oligomers on the ionomers was observed in both the Cs and Ba systems; however, the results were particularly dramatic in the Cs system.

The reader is reminded that biphasic ionomers are characterized by a morphology which depends on ionic group aggregation: aggregates of ionic groups form multiplets, and aggregates of multiplets form clusters. According to the Eisenberg-Hird-Moore (EHM) model of ionomer morphology,<sup>5</sup> the chain segments surrounding the multiplets, within a radius which is thought to be related to the persistence length of the polymer, are restricted in mobility; this gives rise to the cluster phase ("hard phase") with a higher glass transition temperature ( $T_g$ ) than that of the matrix ("soft phase"). The two  $T_g$ 's are typically detected by dynamic mechanical analysis (DMA). A broad small-angle X-ray scattering (SAXS) peak is also generally observed in biphasic ionomers and is interpreted by the EHM model as the most prevalent distance between multiplets.

In the blends of the carboxylated polystyrene ionomers with the short, monofunctional oligomers, both  $T_g$ 's are plasticized by the Ba oligomer; in the Cs system, in contrast, the cluster  $T_g$  is first strongly plasticized and then disappears, along with the SAXS peak, upon the addition of 5 wt % oligomer to the ionomer. This is attributed to the relative weakness of the ionic interactions in the Cs system, such that the cluster morphology is easily disturbed and destabilized by the plasticizing oligomer molecules. A new SAXS peak which appears for Cs oligomer contents of 20 wt % and above indicates the formation of a new morphology, suggested to be micelles (or inverted multiplets) of the oligomer within the ionomer matrix.<sup>4</sup>

In this paper, we present a study of similar blends where, this time, the length of the oligomer chains is greater than the average segmental length between ionic groups in the ionomer. In other words, the ion

\* To whom correspondence should be addressed.

<sup>†</sup> Université Laval.

<sup>‡</sup> Université de Liège.

© Abstract published in *Advance ACS Abstracts*, June 15, 1995.

**Table 1. Characteristics of the Oligomers Synthesized, Where  $f$  is the Functionality and  $n$  the Number of Styrene Units per Chain**

product	$\bar{M}_w$	$\bar{M}_w/\bar{M}_n$	$f$	$n$
$\alpha$ -carboxystyrene (S21-CAH)	2200	1.1	0.97	21
$\alpha,\omega$ -dicarboxystyrene (S42- $\alpha,\omega$ CAH)	4400	1.1	1.94	42

**Table 2. Glass Transition Temperatures of the Neutralized Oligomers, as Determined by DSC**

oligomer	$T_g$ ( $^{\circ}\text{C} \pm 2$ )
S21-CACs	87
S21-CABa	90
S42- $\alpha,\omega$ CACs	101
S42- $\alpha,\omega$ CABa	105
S48- $\alpha,\omega$ CABa	104 <sup>a</sup>

<sup>a</sup> Reference 7.

content of the oligomers is less than that of the ionomers. Specifically, carboxylated polystyrene ionomers of 7 and 10 mol %, neutralized by Cs and Ba, are blended with two kinds of functionalized oligomers. One is an oligomer of 21 styrene units functionalized at one end only by the appropriate (Cs or Ba) carboxylate moiety. The other oligomer is composed of 42 styrene units functionalized at both ends by the carboxylate moiety. Thus, the two oligomers have, in fact, the same ion content (almost 5 mol %), but their chain lengths correspond to roughly 2 and to 3–4 times, respectively, the average segmental length between ionic groups in the ionomers. They are also about an order of magnitude longer than the estimated persistence length of polystyrene.

## Experimental Section

The styrene oligomers were synthesized in THF by classical anionic techniques.<sup>6,7</sup> Initiation of the monofunctional oligomer was effected by activating  $\alpha$ -methylstyrene using *sec*-butyllithium; the bifunctional oligomer was initiated by a styryl dicarbanion prepared using sodium naphthalene. The living chains were terminated with carboxylic acid by bubbling dry  $\text{CO}_2$  through the reaction mixture and acidifying. The oligomers were recuperated by precipitation in  $\text{MeOH}/\text{H}_2\text{O}$  (80/20, v/v) and drying at 60  $^{\circ}\text{C}$  under reduced pressure for 48 h.

The molecular weight,  $\bar{M}_w$ , and polydispersity,  $\bar{M}_w/\bar{M}_n$ , of the oligomers (determined by size-exclusion chromatography), their functionality,  $f$  (determined by titration with a standardized solution of NaOH in MeOH using phenolphthalein as the indicator and knowing the molecular weight), and the number,  $n$ , of styrene units per chain are given in Table 1. Neutralization of the acid groups into Cs and Ba salts was accomplished in benzene/methanol (90/10, v/v) solutions, to which calculated amounts (to a 10% excess) of standardized solutions of the respective hydroxide in methanol were added. The neutralized oligomers were then recovered by precipitation in methanol and were dried at 60  $^{\circ}\text{C}$  under reduced pressure for 2 weeks. The glass transition temperatures of the Cs and Ba oligomers, determined by differential scanning calorimetry (Perkin-Elmer DSC-4) at 20  $^{\circ}\text{C}/\text{min}$ , are given in Table 2, with a value from the literature<sup>7</sup> included for comparison.

The poly(styrene-co-styrenecarboxylic acid) (PS-SCA) copolymers were obtained through chemical modification of polystyrene, following the recipe of Hird and Eisenberg.<sup>8</sup> The polystyrene used was synthesized in the laboratory by classical free-radical techniques and determined to have a molecular weight ( $\bar{M}_w$ ) of 100 000 and a polydispersity of 2.0. Following the carboxylation procedure and purification, the copolymers were dried at 60  $^{\circ}\text{C}$  under reduced pressure for a week. Size-exclusion chromatography of the final product indicated that the molecular weight was unaffected by the reaction. Copolymers of two acid contents were prepared, determined by titration to be 6.9 and 9.9 mol %, respectively. These copolymers will henceforth be referred to as 7 and 10% copolymers.

Neutralization, recuperation, and drying of the corresponding Cs and Ba ionomers (PS- $x$ SCA-Cs and PS- $x$ SCA-Ba, where  $x$  indicates the molar fraction of ionic groups) were accomplished in the same way as for the oligomers.

The blends were prepared by dissolving calculated amounts of the components in benzene/methanol (90/10, v/v) to give about 1% (w/v) solutions, which were stirred for about 12 h, then freeze-dried, and further dried at 60  $^{\circ}\text{C}$  under reduced pressure for 2 weeks. They were subsequently compression-molded into the desired form at about 100  $^{\circ}\text{C}$  above their estimated  $T_g$ , under a pressure of about 10 MPa for about 20 min. Following molding, the samples were kept in a desiccator containing  $\text{P}_2\text{O}_5$  until used. All blends were transparent.

Dynamic mechanical thermal analysis was performed using the Polymer Laboratories DMTA, Mk II, in both dual cantilever bending mode and shear mode. The measurements were made at five frequencies (0.3, 1, 3, 10, and 30 Hz) and a deflection of 64  $\mu\text{m}$ , at a heating rate of 1  $^{\circ}\text{C}/\text{min}$ . The sample chamber was constantly flushed with a light flow of dry nitrogen. For the bending mode, rectangular bars of dimensions 35  $\times$  10  $\times$  2 mm, giving a free length of 5 mm when clamped, were used. For the shear mode, twin disks of 12-mm diameter and 2.5-mm thickness were used; these were obtained by remolding the rectangular bars after the bending mode measurements. All of the data reported, except activation energies, are for a frequency of 1 Hz.

Small-angle X-ray scattering measurements at ambient temperature were taken with a Rigaku 12-kW rotating anode, using Ni-filtered Cu K $\alpha$  radiation ( $\lambda = 0.154$  nm), a Rigaku-Denki small-angle camera under vacuum, and a Rigaku scintillation counter detector. The beam was collimated by two slits of widths 0.16 and 0.12 mm. The sample-to-detector distance was 200 mm. The samples were in the form of disks of 12-mm diameter and 1-mm thickness, obtained by further molding of the samples used for DMTA analysis. The time of exposure of the samples was about 3 h. Since the X-ray analyses were for qualitative purposes, the only correction made to the profiles obtained was a subtraction of that obtained for pure polystyrene.

## Results and Discussion

**Pure Ionomers.** It is observed, first of all, that the Cs and Ba ionomers have all the characteristics of typical biphasic ionomers. This is illustrated in Figure 1. The ionomers show two transitions, assigned as usual to the matrix and cluster glass transitions and which we will call  $T_{g1}$  and  $T_{g2}$ , respectively. Compared to the intensity of the loss tangent maximum for the acid form, that for  $T_{g1}$  of the ionomers is considerably diminished and decreases as the ion content is increased; the maximum for  $T_{g2}$  increases with ion content. The temperature of the maximum increases with ion content for both transitions. Corresponding changes are observed in the modulus curves.

Second, it is noteworthy that the intensity of  $T_{g1}$  in the 7% ionomers is significantly greater than that of  $T_{g2}$ , whereas the opposite is true in the 10% ionomers. This also seems to be the case if the area under the peaks is considered (these observations cannot be quantified because of baseline uncertainty, particularly in the  $T_{g2}$  region). This indicates<sup>9</sup> that the volume fraction of the matrix phase is greater than that of the cluster phase in the 7% ionomer but smaller in the 10% ionomer. It may also be noted that, at the same ion content, the intensity of the  $T_{g1}$  maximum is a little higher for the Cs ionomer than for the Ba ionomer (even taking into account overlap from the  $T_{g2}$  maximum), which suggests that the unclustered phase for the former has a somewhat greater volume fraction than that for the latter.<sup>9</sup> This is supported by a higher rubbery modulus,  $E'_r$ , for the Ba ionomer than for the Cs ionomer (whether determined at the minimum

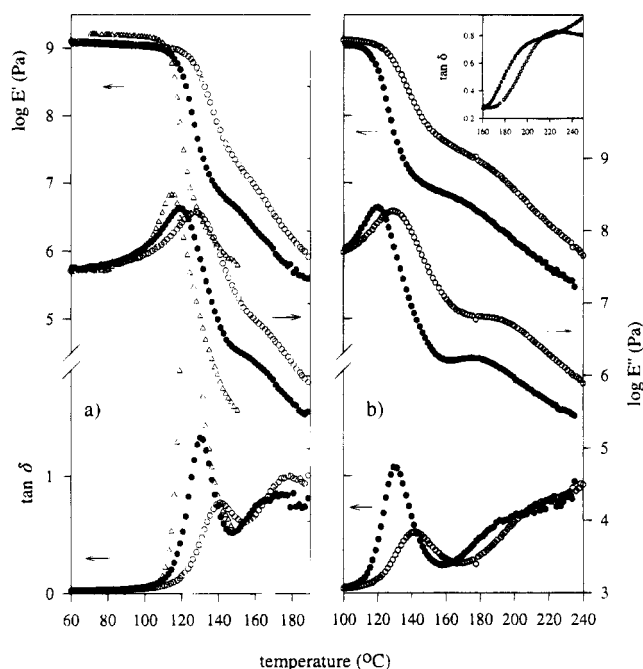


**Figure 1.** Young's storage and loss moduli and loss tangent (1 Hz) as a function of temperature for 7 (●) and 10 (○) mol % carboxylated polystyrene ionomers neutralized by (a) Cs and (b) Ba. The 7 mol % acid precursor ( $\Delta$ ) is also shown in part a. The inset in (b) is shear mode data.

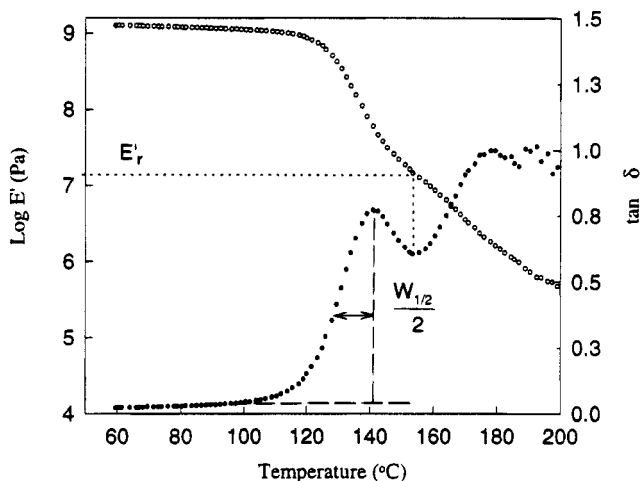


**Figure 2.** Method used to determine the half-widths ( $W_{1/2}$ ) and equilibrium moduli ( $E'_r$ ) from the tensile data.

between the two  $T_g$ 's in the loss tangent curves, as shown in Figure 2, or by the inflection point in the storage modulus curves marking the transition between the rubbery plateaulike and rubbery flowlike regions<sup>9,14</sup>). It can be noted, incidentally, that the loss tangent maxima for  $T_{g2}$  in Figure 1 are not as well-defined as is sometimes observed in the literature for other ionomers. This is probably related to the moderate molecular weight of the ionomers, for it has been shown recently<sup>10</sup> that the clarity of the cluster transition depends, in part, on the molecular weight of the sample: the lower the molecular weight, the more the flow region masks the cluster transition.

Third, whereas  $T_{g1}$  is almost identical in temperature at the same ion content in the Cs and Ba ionomers,  $T_{g2}$  is much higher for the Ba ionomer than for the Cs ionomer. Furthermore, the increase in  $T_{g2}$  with ion content is apparently greater for Ba than for Cs. Evidently, the ionic interactions in the Ba ionomer are

much stronger than those in the Cs ionomer, leading to much more thermally stable multiplets and hence a higher  $T_g$  for the cluster phase in the former. Analogous effects were noted in halatotelechelic polybutadiene carboxylates.<sup>11</sup> As explained in our previous paper,<sup>4,12</sup> this is attributed to both the size and valence of the counterions. Not only does the smaller size of  $Ba^{2+}$  (1.34 Å compared to 1.67 Å for  $Cs^+$ ) result in stronger electrostatic interactions but also its divalence gives rise to effective cross-links, involving ion triplets and their aggregates, that are both ionic and dipolar in nature. The monovalence of  $Cs^+$ , on the other hand, leads to dipolar interactions only among ion pairs; furthermore, these dipolar interactions are relatively weak due to the larger size of the Cs cation. The glass transition temperatures observed for the Cs and Ba ionomers are comparable to those observed for carboxylated ionomers neutralized by Zn and Na, respectively.<sup>13,14</sup>  $Na^+$ , although monovalent, is much smaller in size (0.99 Å) than  $Cs^+$  and thus has a higher charge density, leading to significantly stronger dipolar attractive forces.  $Zn^{2+}$  is known to have some covalent bonding character, which leads to weaker electrostatic associations.<sup>1,13</sup>

Small-angle X-ray scattering of the Cs and Ba ionomers results in the usual broad "ionomer peak", whose maximum is found at almost identical scattering angles for all four ionomers studied, irrespective of the ion content and of the counterion—namely, at  $2\theta = 3.0^\circ$  for the 7% ionomers and at  $2\theta = 2.9^\circ$  for the 10% ionomers, corresponding to Bragg distances of 29 and 30 Å, respectively. This compares well with the results of Hird and Eisenberg<sup>14</sup> and Tomita and Register,<sup>13</sup> who obtained a Bragg distance of 31 Å for the same ionomers neutralized by Na and Zn. The results confirm previous observations<sup>5,13</sup> that the SAXS maximum generally depends little on either the ion content or the metal counterion in bulk ionomers.

**Blends of Ionomers and Oligomers. General Observations of Dynamic Mechanical Results.** A typical series of dynamic mechanical results are shown in Figure 3 for blends of the 10% Cs ionomer with the monofunctional Cs oligomer. The various parameters derived from these curves, and those for the other blends, are collected in Tables 3–6. It is to be noted that the parameters determined for the matrix transition are obtained from DMTA tensile mode data and those for the cluster transition from shear mode data, all at 1 Hz. The molar ratio,  $R$ , of oligomer ionic groups to ionomer ionic groups for each weight composition studied is given for comparison. The intensities (loss tangent maxima) of the two glass transition temperatures,  $T_{g1}$  and  $T_{g2}$ , are represented by  $\tan \delta_{m1}$  and  $\tan \delta_{m2}$ , respectively. Since they are used solely for qualitative purposes, baselines were not subtracted from the intensities. Because baseline subtraction is particularly uncertain for  $T_{g2}$  due to overlap of the flow region, half-widths ( $W_{1/2}$ ) were determined for  $T_{g1}$  only. As shown in Figure 2,  $W_{1/2}$  was determined from the first half of the transition, supposing that the loss tangent peak is symmetric, that there is no significant increase in baseline, and that there is no significant overlap in this region from the higher temperature transition; although none of these conditions are completely true, we consider that the errors introduced are not very large and do not compromise the qualitative comparisons to be made.  $T_{g,Fox}$  was calculated using the Fox equation,<sup>15</sup> given for comparison because it frequently describes the  $T_g$  variation of plasticized poly-

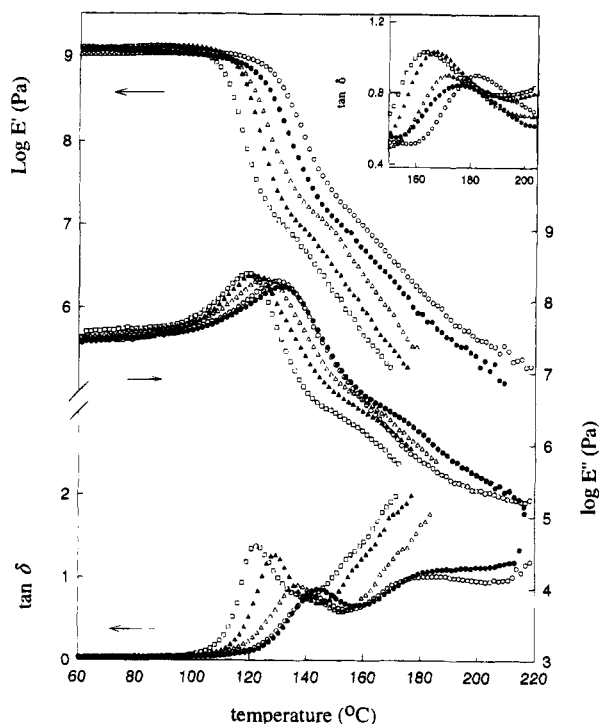


**Figure 3.** Young's storage and loss moduli and loss tangent (1 Hz) as a function of temperature for the 10% ionomer/monofunctional oligomer Cs blends of 100/0 (○), 90/10 (●), 80/20 (△), 60/40 (▲), and 40/60 (□) weight ratios. The inset gives the shear loss tangent data for the same blends.

mers (in the calculations, 15 °C was added to the oligomer  $T_g$ 's of Table 2 to account for the difference we generally observe between DSC and DMTA values under the measurement conditions used<sup>16</sup>). The rubbery moduli,  $E'_r$ , were determined from the minimum in the tensile loss tangent curves, as illustrated in Figure 2. Apparent Arrhenius activation energies,  $H(A)_1$  and  $H(A)_2$ , for the two transitions, obtained from the  $\tan \delta$  maxima at the five frequencies used, are also included in the tables.

The variations of the  $T_g$  maxima as a function of oligomer content are shown in Figure 4. It is observed, first of all, that the biphasic morphology remains present for all of the compositions studied. In general, the plasticizing effects of either oligomer on either  $T_g$  are relatively small and, for  $T_{g1}$ , tend to be less than that predicted by the Fox equation (see the tables). Furthermore, there are no striking differences between the Cs and Ba systems, in contrast to what was observed previously<sup>4</sup> (see the Introduction) for blends with the short, monofunctional oligomers. Interestingly, as (long) monofunctional oligomer is added to the ionomers, the difference in  $T_{g1}$  between the 7 and 10% ionomer blends becomes attenuated (Figure 4a). This is also true for  $T_{g2}$  in the Cs system.  $T_{g2}$  in the Ba system appears unaffected for both ionomers (although a clear maximum could not be determined for the 7% Ba ionomer blends). This small difference between the Cs and Ba systems is probably related, at least in part, to the greater strength of the electrostatic interactions in the Ba system compared to the Cs system, as was observed in ref 4 and as summarized in the Introduction. However, in contrast to the short oligomers, the long, monofunctional oligomers have only a mild, plasticizing effect on the ionomers since, due to their greater length, they introduce much less additional free volume to the blends than their shorter counterparts. Other trends

occur for the bifunctional oligomers, which will be referred to shortly.

As far as the intensities of the loss tangent maxima are concerned, it can be observed from the tables that, in the systems with the monofunctional oligomer, that of  $T_{g1}$  tends to increase with oligomer content, suggesting an increase in the volume fraction of the unclustered phase. This indicates that the monofunctional oligomers participate more in the matrix phase than in the cluster phase of the ionomer. The intensities of the  $T_g$ 's in the systems with the bifunctional oligomer appear to be little affected. In most cases, the half-width of  $T_{g1}$  also tends to increase with oligomer content, indicating some increase in the compositional heterogeneity of this phase. The activation energy for  $T_{g1}$  generally decreases with oligomer content, whereas it remains constant within experimental error for  $T_{g2}$ . As is usual for ionomers,<sup>9,14,17</sup> the former is always greater than the latter. In most of the systems, but not all, there is also a tendency for the rubbery modulus to decrease with added oligomer.

**Antiplasticization Effect.** In the ionomer/oligomer blends involving the bifunctional oligomers, two particularly significant observations can be made. The first is an antiplasticization effect on  $T_{g1}$  which is evident at low oligomer contents in the 7% ionomer. It can be seen in Figure 4b that  $T_{g1}$  occurs at higher temperatures for the ionomers plasticized by 10 and 20 wt % oligomer than for the pure ionomers. This is especially pronounced for the Ba ionomer. Of the compositions studied, this effect is greatest at 20 wt % oligomer for the Cs system and at 10 wt % oligomer for the Ba system. The rubbery modulus in the Ba system is also apparently greater at 10 and 20 wt % oligomer content than for the pure ionomer (Table 5).

A possible explanation for the antiplasticization effect is that relatively low amounts of oligomer cause an increase in dispersion of ionomer ionic groups in the matrix phase, but without reducing the strength of the ionic aggregates. In bulk ionomers, it is known that the greater the dispersion of ionic groups in the matrix phase, the higher the  $T_g$  of this phase.<sup>16</sup> This situation may occur with the bifunctional oligomers as long as their concentration is such that both of their terminal segments are "pinned" in ionic aggregates (multiplets) made up primarily of ionomer ionic groups, thus preventing the oligomers from acting as plasticizers. These aggregates may be in the matrix phase, but it is also possible that they be located within the cluster phase (near their boundaries with the matrix), so that much of the styrene chain can be looped within the matrix phase. This may explain the little change in relative loss intensities observed for the two  $T_g$ 's in these systems (Table 5). In any case, the length of these oligomers, an order of magnitude greater than the estimated persistence length of polystyrene, not only permits them to participate in two neighboring aggregates without undue strain but also favors a preference of the nonionic portion for the matrix phase where there are larger styrene domains to accommodate them. At higher oligomer contents, the low molecular weight nature of the oligomer chains, with their lower  $T_g$ , must necessarily prevail and cause some plasticizing action, as observed.

**Phase Separation.** The second observation concerns the fact that the two  $T_g$ 's in the 10% ionomers are practically unaffected by the presence of the bifunctional oligomers (Figure 4b and Table 6); this is particularly

**Table 3. Various Parameters Determined from Dynamic Mechanical Thermal Analysis for the Cs and Ba Blends of the 7% Ionomer with the Monofunctional Oligomer (See Text for Details)**

blend	<i>P</i> (%)	<i>R</i>	<i>T</i> <sub>g1</sub> (°C ± 2)	<i>T</i> <sub>g,Fox</sub> (°C)	tan δ <sub>m1</sub> (±0.1)	<i>W</i> <sub>1/2</sub> (°C ± 2)	<i>H</i> (A) <sub>1</sub> (kJ/mol ± 30)	log <i>E'</i> <sub>r</sub> (Pa ± 0.1)	<i>T</i> <sub>g2</sub> (°C ± 4)	tan δ <sub>m2</sub> (±0.1)	<i>H</i> (A) <sub>2</sub> (kJ/mol ± 30)
PS-0.07SCA-Cs/S21-CACs	100/0	0.00	130		1.3	15	510	6.7	170	0.8	220
	90/10	0.08	131	127	1.3	19	480	6.6	168	0.8	230
	80/20	0.17	126	124	1.4	20	420	6.5	166	0.8	230
	60/40	0.45	123	118	1.4	21	400	6.5	165	0.9	210
	40/60	1.01	121	113	1.6	22	410	6.5	160	0.9	200
PS-0.07SCA-Ba/S21-CABa	100/0	0.00	131		1.1	16	520	6.9	<i>a</i>	<i>a</i>	<i>a</i>
	90/10	0.08	132	128	1.0	18	460	6.9	<i>a</i>	<i>a</i>	<i>a</i>
	80/20	0.17	127	125	1.0	20	430	6.7	<i>a</i>	<i>a</i>	<i>a</i>
	60/40	0.45	125	120	1.2	22	410	6.4	<i>a</i>	<i>a</i>	<i>a</i>
	40/60	1.01	122	115	1.4	24	420	6.3	<i>a</i>	<i>a</i>	<i>a</i>

<sup>a</sup> Impossible to determine.**Table 4. Various Parameters Determined from Dynamic Mechanical Thermal Analysis for the Cs and Ba Blends of the 10% Ionomer with the Monofunctional Oligomer (See Text for Details)**

blend	<i>P</i> (%)	<i>R</i>	<i>T</i> <sub>g1</sub> (°C ± 2)	<i>T</i> <sub>g,Fox</sub> (°C)	tan δ <sub>m1</sub> (±0.1)	<i>W</i> <sub>1/2</sub> (°C ± 2)	<i>H</i> (A) <sub>1</sub> (kJ/mol ± 30)	log <i>E'</i> <sub>r</sub> (Pa ± 0.1)	<i>T</i> <sub>g2</sub> (°C ± 4)	tan δ <sub>m2</sub> (±0.1)	<i>H</i> (A) <sub>2</sub> (kJ/mol ± 30)
PS-0.10SCA-Cs/S21-CACs	100/0	0.00	141		0.8	22	590	7.2	185	0.9	260
	90/10	0.05	142	137	0.9	22	530	6.8	177	0.9	260
	80/20	0.12	137	133	1.0	22	500	6.6	172	0.9	250
	60/40	0.33	129	124	1.3	17	480	6.6	167	1.0	220
	40/60	0.74	122	117	1.4	15	440	6.5	163	1.0	200
PS-0.10SCA-Ba/S21-CABa	100/0	0.00	142		0.5	25	540	7.5	225	0.8	220
	90/10	0.05	137	138	0.6	29	480	7.2	220	0.8	220
	80/20	0.12	137	134	0.6	30	470	7.0	225	0.8	220
	60/40	0.33	131	126	0.7	36	410	6.9	225	0.8	210
	40/60	0.74	123	119	0.9	35	350	6.2	225	0.8	210

**Table 5. Various Parameters Determined from Dynamic Mechanical Thermal Analysis for the Cs and Ba Blends of the 7% Ionomer with the Bifunctional Oligomer (See Text for Details)**

blend	<i>P</i> (%)	<i>R</i>	<i>T</i> <sub>g1</sub> (°C ± 2)	<i>T</i> <sub>g,Fox</sub> (°C)	tan δ <sub>m1</sub> (±0.1)	<i>W</i> <sub>1/2</sub> (°C ± 2)	<i>H</i> (A) <sub>1</sub> (kJ/mol ± 30)	log <i>E'</i> <sub>r</sub> (Pa ± 0.1)	<i>T</i> <sub>g2</sub> (°C ± 4)	tan δ <sub>m2</sub> (±0.1)	<i>H</i> (A) <sub>2</sub> (kJ/mol ± 30)
PS-0.07SCA-Cs/S42-α,ω-CACs	100/0	0.00	130		1.3	15	510	6.7	170	0.8	220
	90/10	0.07	133	128	1.3	16	490	6.6	162	0.7	260
	80/20	0.17	135	127	1.3	19	510	6.5	164	0.7	250
	60/40	0.45	130	124	1.2	21	480	6.4	<i>a</i>	<i>a</i>	<i>a</i>
	40/60	1.01	125	121	1.2	22	490	6.2	<i>a</i>	<i>a</i>	<i>a</i>
PS-0.07SCA-Ba/S42-α,ω-CABa	100/0	0.00	131		1.1	16	520	6.9	<i>a</i>	<i>a</i>	<i>a</i>
	90/10	0.07	142	130	0.7	20	600	7.3	200	0.7	200
	80/20	0.17	138	129	0.7	20	580	7.2	200	0.7	220
	60/40	0.45	130	126	0.9	22	500	6.9	190	0.7	210
	40/60	1.01	123	124	1.0	24	450	6.9	195	0.7	210

<sup>a</sup> Impossible to determine.**Table 6. Various Parameters Determined from Dynamic Mechanical Thermal Analysis for the Cs and Ba Blends of the 10% Ionomer with the Bifunctional Oligomer (See Text for Details)**

blend	<i>P</i> (%)	<i>R</i>	<i>T</i> <sub>g1</sub> (°C ± 2)	<i>T</i> <sub>g,Fox</sub> (°C)	tan δ <sub>m1</sub> (±0.1)	<i>W</i> <sub>1/2</sub> (°C ± 2)	<i>H</i> (A) <sub>1</sub> (kJ/mol ± 30)	log <i>E'</i> <sub>r</sub> (Pa ± 0.1)	<i>T</i> <sub>g2</sub> (°C ± 4)	tan δ <sub>m2</sub> (±0.1)	<i>H</i> (A) <sub>2</sub> (kJ/mol ± 30)
PS-0.10SCA-Cs/S42-α,ω-CACs	100/0	0.00	141		0.8	22	590	7.2	185	0.9	260
	90/10	0.05	140	138	0.8	21	470	7.0	190	0.9	270
	80/20	0.12	142	136	0.8	26	440	6.8	200	0.9	250
	60/40	0.33	139	131	0.6	<i>a</i>	420	6.8	195	0.9	280
	40/60	0.74	<i>a</i>	126	<i>a</i>	<i>a</i>	460	6.4	190	0.9	260
PS-0.10SCA-Ba/S42-α,ω-CABa	100/0	0.00	142		0.5	25	540	7.5	225	0.8	220
	90/10	0.05	142	140	0.5	30	620	7.2	225	0.7	240
	80/20	0.12	140	137	0.5	40	560	7.0	225	0.8	230
	60/40	0.33	139	133	0.5	<i>a</i>	500	6.8	225	0.8	230
	40/60	0.74	<i>a</i>	128	<i>a</i>	<i>a</i>	460	6.4	230	1.1	220

<sup>a</sup> Impossible to determine.

evident for the Ba system (in the Cs system, *T*<sub>g2</sub> seems to go through a maximum at about 20 wt % oligomer content). Loss tangent curves for these systems are shown in Figure 5. From these, it is evident that there is macrophase separation in the two systems, which explains the lack of influence of the oligomer on the *T*<sub>g</sub>'s of the ionomers. A new loss tangent peak appears at

about 117 °C with increasing oligomer content, about 15 °C higher than the *T*<sub>g</sub>'s measured by DSC for the bifunctional oligomers (Table 2); since this corresponds to the difference that we generally observe between the DSC and DMTA analyses, we conclude that the transition at 117 °C represents essentially pure, phase-separated oligomer.

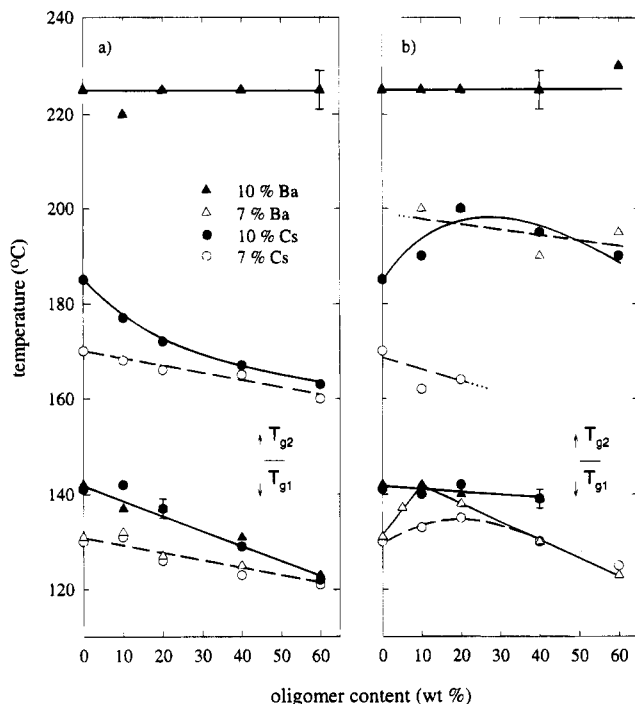


**Figure 4.** Glass transition temperatures of the matrix ( $T_{g1}$ ) and cluster ( $T_{g2}$ ) phases of the blends of the (a) monofunctional and (b) bifunctional oligomers with the ionomers indicated. The error bars shown apply to all of the points for  $T_{g1}$  and  $T_{g2}$ , respectively.

It seems that, at 10% ion content where the matrix phase is smaller in volume than the cluster phase, the matrix (ion-poor) regions have become too small to accommodate the styrene portion of the bifunctional oligomer chains, which are 4 times the average segmental length between ionic groups in the ionomer. In contrast, the styrene domains in the 7% ionomer, where the bifunctional oligomer is about 3 times as long as the ionomer segments and where the volume fraction of the matrix phase is greater than that of the cluster phase, are apparently still large enough to accommodate the oligomer; there is no hint of phase separation in the loss tangent curves for these blends.

For comparison, the loss tangent curves of the 10% Ba ionomer blends with the monofunctional oligomer are also shown in Figure 5. Although this cannot be stated with certainty, there is some evidence, from the increasing width of the curves with oligomer content and some asymmetry in the curve for the 60/40 blend, that there may be nascent phase separation in these blends, too; this was not observed in the corresponding Cs blends. This may be another indication that the volume fraction of the matrix phase in the Ba ionomer is a little smaller than that in the Cs ionomer, as suggested by Figure 1. It also suggests that it is the interplay between the length of the oligomer chains and the amount and size of the matrix domains that primarily determines the miscibility (at the level detectable by DMTA) of chemically identical ionomer/functionalized oligomer blends and that their functionality (whether mono- or bifunctional) plays a secondary role.

It is worth mentioning that macrophase separation between the two components does not rule out interfacial interactions, in particular among the carboxylate groups of the two components. It should also be emphasized that the miscibility observed in most of the above systems is at a level detectable by DMTA. Microphase separation of the components at a local

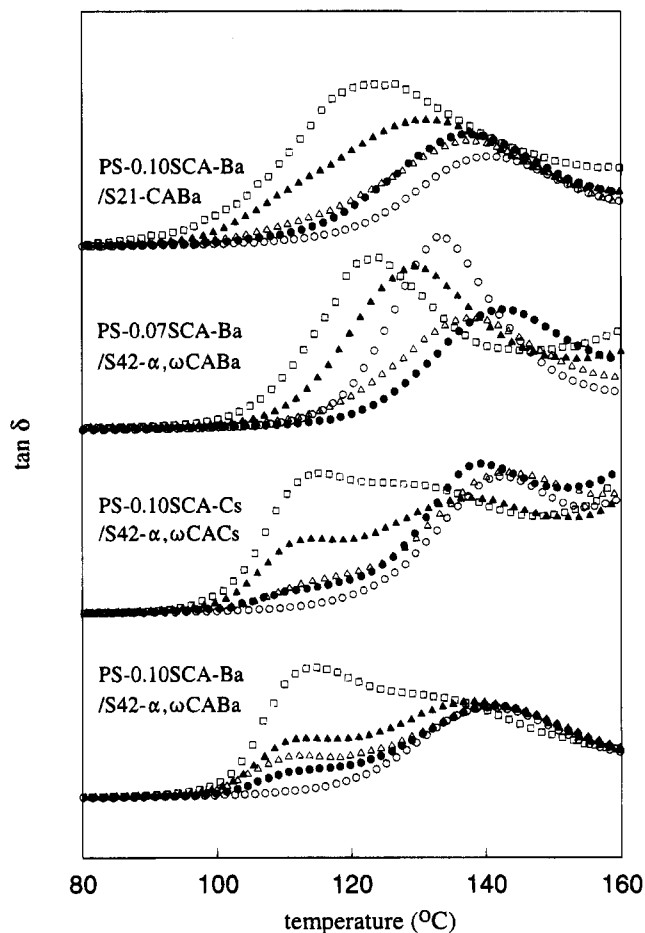


**Figure 5.** Tensile loss tangent curves (1 Hz) of the ionomer/oligomer blends indicated at weight ratios of 100/0 (○), 90/10 (●), 80/20 (△), 60/40 (▲), and 40/60 (□).

level, into domains too small to be detected by DMTA, may well be present. In this case, one could invoke the existence of a mixed phase of ionomer and oligomer microdomains (rather than a completely miscible system), probably with extensive carboxylate group interactions and with styrene segment interpenetration to the extent possible locally. Because the ionic aggregates are distributed randomly in the ionomer matrix, which results in variable degrees of local miscibility with the oligomer, the mixed ionomer/oligomer phase may be quite disordered in nature. Moreover, from this point of view, the nascent phase separation which seems to be present in the PS-0.10SCA-Ba/S21-CABa system may be the result of microdomains having a size that it just detectable by DMTA; where there is macrophase separation, the oligomer domains are larger than the minimal size detectable by DMTA.

**Small-Angle X-ray Scattering.** Finally, for all four systems, the ionomer peak in SAXS decreases in intensity and then disappears as the oligomer content in the blend increases. There is little change in the position of the peak, however. As indicated in Table 7, the peak is absent for all blend compositions studied for three of the four Cs systems; for the 10% Cs ionomer blended with the monofunctional oligomer, the peak is still evident at 10 and 20 wt % oligomer content. In the Ba systems, it tends to disappear at higher oligomer contents than for the corresponding Cs systems. The SAXS peak is still present at 10 and 20% oligomer content and at 10, 20, and 40% oligomer contents in the 7 and 10% Ba ionomer/monofunctional oligomer blends, respectively. In the Ba ionomer/bifunctional oligomer

**Table 7. Presence of an Ionomer Peak in Small-Angle X-ray Scattering Curves in the Ionomer/Oligomer Blends: (+) Observed; (○) Not Observed**

oligomer (wt %)	7% ionomer		10% ionomer	
	Cs	Ba	Cs	Ba
S21				
0	+	+	+	+
10	○	+	+	+
20	○	+	+	+
40	○	○	○	+
60	○	○	○	○
S42				
0	+	+	+	+
10	○	+	○	○
20	○	○	○	○
40	○	○	○	○
60	○	○	○	○

blends, the SAXS peak is present only for the 7% ionomer at 10% oligomer content. There also seems to be a general tendency in all but the phase-separated blends for the small-angle upturn at scattering angles below  $1^\circ$  ( $2\theta$ ) to decrease slightly to lower angles.

Some of the decrease in intensity can be accounted for simply by the addition of the oligomer because it has a lower ion content; in other words, adding oligomer causes the Ba content to decrease which, in turn, decreases the intensity of the SAXS peak. However, this dilution effect should be similar for all of the systems. Anything affecting the ionic aggregate structure, including a greater dispersion of the ionic groups into the styrene matrix, less well-defined ionic cores, and any changes in the size and number of the contributing aggregates, must account for the rest. There are, unfortunately, no apparent correlations between the composition at which the SAXS peak disappears and the information deduced above from the dynamic mechanical properties, to guide us in interpreting the SAXS data. On the other hand, the absence of a SAXS peak, but presence of two  $T_g$ 's in dynamic mechanical data, was also observed by Douglas et al.<sup>18</sup> for Zn blends of partially sulfonated polystyrene with poly(styrene-co-vinylpyridine) copolymers. This can be explained, in terms of the EHM model, as due to the breakup of larger aggregates into smaller ones that are still sufficiently rigid to leave a cluster phase intact, but too small to cause significant X-ray scattering.<sup>19</sup> For our systems, this explanation alone seems too simplistic, as a breakup into smaller aggregates that still scatter X-rays, at the lower oligomer contents, would be expected to be accompanied by an increase in the scattering angle of the SAXS maximum (which is not what is observed) to reflect the greater number of scattering centers and hence smaller average distance between them. One could perhaps evoke the possibility that, whatever their number, the multiplets disperse themselves in such a way as to always maintain a certain preferred distance within a given matrix, in which case the peak simply decreases in intensity without changing position as the aggregates become smaller with added oligomer; a similar explanation was suggested to account for the little change observed in SAXS peak position with change in the composition of blends of polystyrene and short, monofunctional oligomers.<sup>4</sup> Other explanations are no doubt possible; for example, the disordered mixed phase mentioned above may somehow eliminate any preference in the distances between ionic aggregates. In any case, definitive explanations will require more detailed X-ray (and perhaps other) analyses.

As a final remark, one might have expected, in the macrophase-separated systems, that the ionomer SAXS peak would be maintained to higher oligomer contents than for the other systems, possibly superposed by a peak arising from the oligomer phase. Since this is not observed, we must conclude that, despite the phase separation between the components (which may not be complete), the ionic aggregate structure is perturbed just as for the other systems. This may also be consistent with the idea of a disordered mixed phase and the existence of significant interfacial interactions.

## Conclusions

It has been shown that plasticization of biphasic ionomers by functionalized oligomers, where the ionomers and oligomers are chemically identical, is determined primarily by the miscibility of the oligomers in either phase of the ionomer. This is related both to how the length (molecular weight) of the nonionic part of the oligomer chain compares to the average length (molecular weight) of the segments between ionic groups in the ionomer and to the extent of interactions between the ionic groups of the two components. Ionic group aggregation, in turn, controls the relative volumes of the matrix and cluster phases of the ionomer, which is thus also a critical factor.

Short, monofunctional oligomers, with high ion content compared to that of the ionomer, were previously shown<sup>4,20</sup> to plasticize both ionomer phases, and when the ionic associations in the ionomer are relatively weak as is the case in the Cs system, they can destroy the cluster phase and even possibly take on micellar characteristics. The longer oligomers of this study do not destroy the biphasic morphology of the ionomers, no doubt because they lack the mobility of the shorter oligomers due to their size, and thus do not strongly reduce the rigidity and strength of the ionic aggregates. However, they do tend to have some mild plasticizing action on both phases, similar in both Cs and Ba systems, and they apparently perturb the ionic aggregate structure enough to strongly affect the ionomer SAXS peak.

Two limiting situations were noted. The first is that, under some conditions, an antiplasticization effect can be observed, attributed to a greater dispersion of ionic aggregates in the matrix phase caused by the presence of the oligomers. This is probably unique to bifunctional oligomers (at low concentrations) whose ends can both be fixed in ionic aggregates dominated by ionomer groups (which prevents plasticizing activity by the oligomers) and whose length is sufficient to permit participation of the nonionic portion in the matrix phase but not enough to provoke phase separation. Thus, it is most likely to occur in ionomers whose matrix phase is more important in volume than the cluster phase.

Second, when the volume fraction of the matrix phase becomes too small to accommodate the nonionic portion of the oligomer chains, macrophase separation occurs. This was observed clearly for the longest oligomers of this study in blends with the ionomer where the cluster phase fraction is greater than the matrix phase fraction. This phenomenon is likely to occur just as well for a monofunctional oligomer of sufficient length, as suggested by the data for another of the blend series studied. As far as the molecular weight parameter is concerned, the parallel with blends of homopolymers and block copolymers and with blends of ionomers and their parent homopolymers is clearly evident here, as



are the consequences for blends of biphasic ionomers of widely different ion contents.

**Acknowledgment.** C.G.B. and M.P. gratefully acknowledge the financial support of NSERC (Canada) and FCAR (Québec) for this research. R.J. is grateful to the "Services Fédéraux des Affaires Scientifiques, Techniques et Culturelles" (S.S.T.C.) for financial support in the framework of the "Pôles d'Attraction Interuniversitaires: Polymères". The "Ministère de l'Enseignement Supérieur et des Sciences du Québec" and the "Communauté Française de Belgique" are acknowledged for providing funds for a cooperative program.

## References and Notes

- (1) Register, R. A.; Bell, T. R. *J. Polym. Sci., Part B: Polym. Phys.* **1992**, *30*, 569. Tomita, H.; Register, R. A. *Macromolecules* **1993**, *26*, 2796.
- (2) Bazuin, C. G.; Rancourt, L.; Villeneuve, S.; Soldera, A. *J. Polym. Sci., Part B: Polym. Phys.* **1993**, *31*, 1431.
- (3) Nyrkova, I. A.; Khokhlov, A. R.; Doi, M. *Macromolecules* **1993**, *26*, 3601.
- (4) Plante, M.; Bazuin, C. G.; Jérôme, R. *Macromolecules* **1995**, *28*, 1567.
- (5) Eisenberg, A.; Hird, B.; Moore, R. B. *Macromolecules* **1990**, *23*, 4098.
- (6) Broze, G.; Jérôme, R.; Teyssié, Ph. *Macromolecules* **1982**, *15*, 920. Vanhoorne, P.; Jérôme, R.; Teyssié, Ph.; Lauprêtre, F. *Macromolecules* **1994**, *27*, 2548.
- (7) Pelzer-Foucart, M. Ph.D. Thesis, Université de Liège, Liège, Belgium, 1988.
- (8) Hird, B.; Eisenberg, A. *J. Polym. Sci., Part A: Polym. Chem.* **1993**, *31*, 1377.
- (9) Hird, B.; Eisenberg, A. *J. Polym. Sci., Part B: Polym. Phys.* **1990**, *28*, 1665. Kim, J.-S.; Wu, G.; Eisenberg, A. *Macromolecules* **1994**, *27*, 814. Kim, J.-S.; Jackman, R. J.; Eisenberg, A. *Macromolecules* **1994**, *27*, 2789.
- (10) Kim, J.-S.; Yoshikawa, K.; Eisenberg, A. *Macromolecules* **1994**, *27*, 6347.
- (11) Broze, G.; Jérôme, R.; Teyssié, Ph. *J. Polym. Sci., Polym. Phys. Ed.* **1983**, *21*, 2205. Horrion, J.; Jérôme, R.; Teyssié, Ph.; Marco, C.; Williams, C. E. *Polymer* **1988**, *29*, 1203.
- (12) Plante, M. Ph.D. Thesis, Department of Chemistry, Laval University, Quebec, Canada, 1993.
- (13) Tomita, H.; Register, R. A. *Macromolecules* **1993**, *26*, 2791.
- (14) Hird, B.; Eisenberg, A. *Macromolecules* **1992**, *25*, 6466.
- (15) Fox, T. G. *Bull. Am. Phys. Soc.* **1956**, *2*, 123.
- (16) Murali, R.; Eisenberg, A. In *Structure and Properties of Ionomers*; Pineri, M., Eisenberg, A., Eds.; NATO Advanced Study Institute Series C198; Reidel Publishing Co.: Dordrecht, The Netherlands, 1987; p 307.
- (17) Villeneuve, S.; Bazuin, C. G. *Polymer* **1991**, *32*, 2811. Tong, X.; Bazuin, C. G. *J. Polym. Sci., Part B: Polym. Phys.* **1992**, *30*, 389. Neagu-Plesu, R.; Bazuin, C. G. *J. Polym. Sci., Part B: Polym. Phys.* **1991**, *29*, 1305.
- (18) Douglas, E. P.; Waddon, A. J.; MacKnight, W. J. *Macromolecules* **1994**, *27*, 4344.
- (19) Eisenberg, A., private communication.
- (20) Kim, J.-S.; Roberts, S. B.; Eisenberg, A.; Moore, R. B. *Macromolecules* **1993**, *26*, 5256.

MA950048A